

LIMNOLOGY and OCEANOGRAPHY



© 2023 Association for the Sciences of Limnology and Oceanography. doi: 10.1002/lno.12487

Nitrogen availability regulates the effects of a simulated marine heatwave on carbon sequestration and phycosphere bacteria of a marine crop

Meijia Jiang, 1 Jason M. Hall-Spencer, 2,3 Lin Gao, 1 Zengling Ma 0,4 Guang Gao 01*

¹State Key Laboratory of Marine Environmental Science and College of Ocean and Earth Sciences, Xiamen University, Xiamen, China

Abstract

Great hope has been pinned on seaweed cultivation as being a potent way of removing CO_2 to reduce rates of sea surface warming and acidification. Marine heatwaves and nitrogen pollution in coastal ecosystems are serious current issues that need to be better understood to inform decision making and policy. Here, we investigated the effects of a simulated heatwave and nitrogen pollution on carbon sequestration by an important seaweed crop species and its phycosphere bacteria. *Gracilaria lemaneiformis* was grown in ambient and high nitrogen conditions (14 and $200 \mu M L^{-1}$). Photosynthetic rate, seaweed biomass and particulate organic carbon accumulation were significantly increased in "high nitrogen-no heatwave" conditions. In "ambient nitrogen heatwave" conditions, the expression of genes related to photosynthesis was down regulated and the seaweeds lost more dissolved organic carbon (DOC) to the surrounding water, resulting in more refractory dissolved organic carbon (RDOC). In "high nitrogen heatwave" conditions, photosynthetic gene expression was upregulated; bacterial abundance was also increased that can explain the reduced DOC and RDOC accumulation. The simulated heatwave reduced bacterial diversity while high nitrogen alleviated this effect. These findings suggest that the economically important alga *G. lemaneiformis* may lose more DOC and RDOC to nearshore waters during marine heatwave events, enhancing carbon sequestration, while nitrogen enrichment has a counteractive effect.

All over the world marine heatwaves are becoming more frequent, intense, and prolonged due to global warming (Gouvea et al. 2017; Oliver et al. 2021) with 2023 set to be the hottest annual ocean surface temperature in human history. In China, the frequency, duration, and mean intensity of marine heatwaves are twice that of the global average (Yao et al. 2020). Marine heatwaves are periods of warming that are characterized

*Correspondence: guang.gao@xmu.edu.cn

Additional Supporting Information may be found in the online version of this article.

Author Contribution Statement: M.J. involved in investigation, methodology, formal analysis, visualization, writing-original draft preparation, writing-reviewing, and editing. J.H.-S. performed methodology, formal analysis, writing-original draft preparation, writing-reviewing, and editing. L.G. involved in methodology, writing-reviewing, and editing. Z.M. involved in writing-reviewing and editing. G.G. involved in conceptualization, methodology, formal analysis, writing-original draft preparation, writing-reviewing and editing, supervision, and funding acquisition.

first by abnormally high ocean temperatures relative to the average seasonal temperature followed by cooling back to normal for a particular region (Hobday et al. 2016). These pulsed warm water events threaten global biodiversity and the provision of marine ecosystem services as they can cause anoxia and kill habitat forming organisms, such as seagrasses and corals (Smale et al. 2019; Brauko et al. 2020; Smith et al. 2023). Marine heatwaves can have severe impacts on seaweed physiological performance and community structure, e.g., leading to the loss of kelp forests and the rapid spread of non-native species (Pecl et al. 2017; Agostini et al. 2021; Gao et al. 2021*b*).

Seaweeds play an essential role in coastal ecosystems, such as the provision of food, a spatial refuge against predators and the cycling of nutrients (Teagle et al. 2017; Gao et al. 2021a). In addition, the huge potential of seaweeds to sequester carbon is attracting increasing global attention as the need for climate mitigation techniques grows more acute (Gao et al. 2022; Ross et al. 2022). Climate change is expected to impact seaweed carbon fixation and export (Wada et al. 2021).

²Marine Institute, University of Plymouth, Plymouth, UK

³Shimoda Marine Research Center, Tsukuba University, Tsukuba, Ibaraki, Japan

⁴Zhejiang Provincial Key Laboratory for Water Environment and Marine Biological Resources Protection, Wenzhou University, Wenzhou, China

Yet, our knowledge about how marine heatwaves affect algal carbon sequestration is very limited. Nitrogen limitation can stunt algal growth and nitrogen enrichment is known to reduce the negative impacts of high temperatures on growth and photosynthesis in the giant kelp *Macrocystis pyrifera* (Fernandez et al. 2020). However, excess nitrogen can cause problematic seaweed blooms (Schmidt et al. 2012; Feng et al. 2023).

Marine dissolved organic carbon (DOC) is a large carbon reservoir (660 Pg C) that contains as much carbon as the Earth's atmosphere (Follett et al. 2014). The DOC production by algae is the main source of marine DOC. Phytoplankton are estimated to release up to half of their fixed carbon into seawater in the form of DOC (Thornton 2014). The initial release of DOC from algae is usually labile that can be used and transformed to refractory DOC (RDOC) by bacteria (Zheng et al. 2019). This RDOC can be stored in the ocean for long periods of time, becoming a component of carbon sequestration (Jiao et al. 2010). Therefore, phycosphere bacteria play an essential role in carbon sequestration capacity of algae. The seaweeds Sargassum spp. export 6-35% of their production offshore as DOC and 56-78% of macroalgal DOC becomes refractory after mineralization by bacteria (Watanabe et al. 2020). Few studies have documented the impacts of marine heatwaves on DOC excretion by seaweeds and its use by phycosphere bacteria. Egea et al. (2022) found that simulated marine heatwaves in summer did not affect net community productivity dominated by the macroalga Caulerpa prolifera but decreased DOC daily fluxes and increased the proportion of RDOC. However, the potential mechanisms remain unknown.

Gracilaria species are found worldwide and are the most commonly used raw material in the food grade agar industry (Meinita et al. 2017). Gracilaria farming is one of the fastestgrowing aquaculture sectors, contributing to 11% of the global seaweed feed-stock supply chain in 2019. Gracilaria species have been successfully farmed worldwide since the 1950s (Mantri et al. 2022). Gracilaria lemaneiformis (Bory) E.Y. Dawson, Acleto, and Foldvik is estimated to have the highest carbon sequestration capacity among cultivated seaweeds species (Gao et al. 2021a). However, how marine heatwaves affect the carbon sequestration capacity of G. lemaneiformis under changing nitrogen conditions remains unclear. We hypothesize that nitrogen availability may regulate the effects of marine heatwaves on production of DOC and its transformation into RDOC by phycosphere bacteria. In this study, G. lemaneiformis was cultured under a simulated marine heatwave and different nitrogen conditions to test this hypothesis.

Material and methods

Seaweed collection

Gracilaria lemaneiformis was collected from a mariculture zone in Ningde, Fujian province of China (119.31°E, 26.39°N) in February 2022. Sediment, epiphytes and small grazers were removed with filtered seawater in the laboratory. The thalli

were cultured at a light intensity of 80 μ mol photons m⁻² s⁻¹ on a 12-h light: 12-h dark cycle in 17°C seawater, to keep conditions similar to that found in February 2022 at the sampling site.

Experimental design

The heatwave scenario was constructed as Hobday et al. (2016) described, running for 4 weeks (Nepper-Davidsen et al. 2019). Our simulated marine heatwave temperatures were set based on local temperature monitoring (Li et al. 2019). Non-heatwave treatments were held at a steady 17°C. In heatwave treatments, temperature was increased from 17°C by 1°C/day from days 1 to 6 until 23°C was reached (temperature-rising period). The heatwave was sustained until day 13 (7 days in total, temperature-maintaining period). From days 13 to 19, the temperature was reduced by 1°C/day until 17°C (temperature-decreasing period). By the end of the heatwave condition, the thalli had a recovery week (7 days in total, recovery period) till day 26. We used three replicate incubators (HP200G-3, Ruihua, China) per treatment.

After 1 week of acclimation to 17°C in natural seawater. 1 g of healthy G. lemaneiformis were randomly assigned into flasks, each including 1 L of 0.22 µm filtered seawater. The thalli were cultured under combinations of no heatwave and simulated heatwave (coded as HW- and HW⁺) and two nitrogen levels (14 and 200 μ mol L⁻¹; coded as ambient nitrogen, AN and high nitrogen, HN). The nitrogen level of natural seawater is defined as ambiwhich $14.202 \, \mu \text{mol L}^{-1} \, \text{NO}_3^$ includes level. $0.004~\mu\mathrm{mol}~\mathrm{L}^{-1}~\mathrm{NO_2}^-$, and $0.279~\mu\mathrm{mol}~\mathrm{L}^{-1}~\mathrm{NH_4}^+$. The high includes 199.912 μ mol L⁻¹ NO₃⁻, level $0.004 \,\mu\text{mol L}^{-1}\,\text{NO}_2^-$ and $0.279 \,\mu\text{mol L}^{-1}\,\text{NH}_4^+$, which was made by adding NaNO₃ to natural seawater. The high nitrogen concentration falls in the range of eutrophic coastal waters by Teichberg et al. (2010), and supplied adequate nitrogen to the seaweed (Fig. S1). The phosphorus concentration was set to $50 \, \mu \text{mol L}^{-1}$ to avoid phosphorus limitation. Half of the culture medium was replaced every 3 days with filtered $(0.22 \, \mu \text{m})$ seawater with 14 or $200 \,\mu\text{mol L}^{-1}\,\text{N}$. This renewing of medium was a compromise of enough nutrient supply and limited change of phycosphere bacteria. In addition, G. lemaneiformis cannot grow well in closed systems without water exchange even when nutrients are replete. The flasks were stirred three times daily (at 9:00 h, 15:00 h, and 21:00 h). To mimic natural environment, the flasks were open to the atmosphere allowing exchange of gasses and microbes over the seawater-air interface. The effect of atmosphere on bacterial communities should be minor since both the simulated heatwave and nitrogen significantly affected the bacterial structure based on the results. At the end of each stage (days 0, 6, 13, 19, and 26), biomass, net photosynthetic rate, respiration rate, phycobiliproteins content, seawater DOC, seaweed POC (particulate organic carbon) and bacterial abundance were measured. Samples for bacterial diversity and transcriptome analyses of *G. lemaneiformis* were collected on days 13 and 26. Given the wide range of parameters measured and logistical limitations, we had to use three replicates per treatment, as is often the case in such studies (Gouvêa et al. 2017; Hong et al. 2017).

Growth and POC content

The fresh weight (FW) of *G. lemaneiformis* was measured and its specific using a scale (BSA124S, Sartorius, Germany). Its specific growth rate (SGR) was calculated as follows: SGR $(d^{-1}) = \ln(W_2/W_1)/(t_2-t_1)$, where W_1 and W_2 were the FW measured at times t_2 and t_1 . For POC analysis, seaweed tissue samples were dried at 65°C for 24 h. A microbalance was used to weigh out around 1 mg of each sample, which was then pelletized and placed inside tin capsules. With the aid of an elemental analyzer, POC content was calculated (Vario EL cube, Elementar, Germany). The accumulation of seaweed POC (mg C g⁻¹ FW) during the culture period was calculated as follows:

POC accumulation =
$$(B_t^*C_t - B_0^*C_0)/B_0$$

where B_t and B_0 mean biomass at time t (days 6, 13, 19, and 26) and day 0, C_t and C_0 mean POC content at time t (days 6, 13, 19, and 26) and day 0.

Net photosynthetic and dark respiration rates

The net photosynthetic rate and dark respiration rate of G. lemaneiformis were estimated using an oxygen electrode (Oxygraph+, Hansatech, UK). The temperature was maintained by a thermostatic circulator (DHX-2005, China) and light provided by a halogen lamp. About 0.05 g (FW) of algae was put into the chamber containing a 2 mL medium. To minimize the effects of mechanical damage, thalli were placed under cultured conditions for about 1 h (Gao et al. 2018). Net photosynthetic rate was estimated as the increase of oxygen content in seawater over a 10 min period, and dark respiration rate was defined as the decrease in oxygen content in seawater in darkness within 10 min. The net photosynthetic and dark respiration rates were expressed as μ mol O_2 g⁻¹ FW h⁻¹.

Phycobiliproteins

About 0.05 g of algal tissue was ground and extracted in 0.1 M PBS buffer, pH 6.8. The homogenates were centrifuged at 10,000g for 20 min. Phycobiliprotein contents [phycocyanin (PC) and phycoerythrin (PE)] were measured by ultraviolet–visible spectrophotometer (TU1810DASPC, PERSEE, China) at 455, 564, and 592 nm, and calculations were performed using the equations of Beer and Eshel (1985).

DOC release by G. lemaneiformis

At different time points 40 mL seawater samples were collected from each container for the evaluation of DOC concentration. The DOC concentration of seawater without thalli was determined as a baseline. DOC samples were filtered through precombusted (450°C for 2 h) GF/F (Whatman, 0.7 μ m) filters and stored at -20°C in Amber Boston Round glass bottles (precombusted at 450°C for 2 h) immediately after collection. DOC concentrations were estimated using a Shimadzu total organic carbon analyzer (TOC-LCPH, Japan) at 680°C following the combustion catalytic oxidation method. DOC release rate was represented by the difference in DOC concentration over a period of 24 h (μ M C gFW⁻¹ d⁻¹).

DOC samples were kept at 17°C in the dark for 2 months to estimate the amount of RDOC left after bacterial breakdown, following Wada et al. (2008) and Gao et al. (2021*c*).

RDOC fraction to total DOC was calculated as follows:

RDOC fraction (%) =
$$(DOCt_2 - DOCt_2')/(DOCt_1 - DOCt_1') \times 100$$

where DOCt₁ and DOCt₂ mean the DOC concentrations in seawater from our treatments before and after a 2-month dark incubation, respectively, and DOCt₁' and DOCt₂' mean the DOC concentrations in seawater without seaweeds growing in it before and after 2-month dark incubation, respectively. DOC and RDOC accumulation (μ M C g⁻¹ FW) were calculated as follows:

$$\begin{split} \mathrm{DOC}_T \left(\mu \mathrm{MCg}^{-1} \mathrm{FWd}^{-1} \right) &= e^{\mathrm{SGR}t \times T} \times [R0 + (Rt - R0) \times T/t] \\ \mathrm{DOC} \, \mathrm{accumulation} \left(\mu \mathrm{MCg}^{-1} \, \mathrm{FW} \right) \\ &= \sum_1^T \, \mathrm{DOC} \, \mathrm{accumulation} \left(\mu \mathrm{MCg}^{-1} \, \mathrm{FW} \, \mathrm{d}^{-1} \right) \\ \mathrm{RDOC} \, \mathrm{accumulation} \left(\mu \mathrm{MCg}^{-1} \, \mathrm{FW} \right) \\ &= \sum_1^T \mathrm{DOC} T \times [F0 + (Ft - F0) \times T/t] \end{split}$$

where DOC_T means DOC release rate at times T (days 1 to 26), SGR_t means the SGR at times t (days 6, 13, 19, and 26), R_0 and R_t mean the DOC release rate on days 0 and t, F_0 and F_t mean the fractions of RDOC on days 0 and t, respectively.

Bacterial abundance

About 2 mL incubated media were collected into sterile tubes and fixed with glutaraldehyde (0.2% final concentration). Samples were stained with SYBR Green I stain (Invitrogen, USA) at 1:10,000 final concentration and held in the dark for 20 min. BD Accuri C6 flow cytometer was used to analyze all samples after incubation and the bacterial abundance was expressed as cells $\rm mL^{-1}.$

Jiang et al.

Bacterial structure and diversity

From each container a 150 mL seawater sample was filtered through a 0.22 µm polycarbonate membrane (Millipore, USA) to collect microorganisms. These microorganism samples were kept at -80°C until DNA was extracted and purified by Majorbio Bio-pharm Technology, Ltd. in Shanghai, China. The V4 region of the bacterial 16S ribosomal RNA gene was amplified by PCR (95°C for 3 min, followed by 30 cycles at 95°C for 30 s, 45°C for 30 s, and 72°C for 45 s, and a final extension at 72°C for 5 min) using barcoded primers 515F (5'-GTGYCAGCMGCCGCGGTAA-3') and 806R (5'-GGACTACNVGGGTWTCTAAT-3'), where a barcode is an eight-base sequence unique for each sample. PCR reactions were performed in a triplicate 20 µL mixture containing 10 ng of template DNA, $4 \mu L$ of $5 \times FastPfu$ Buffer, $0.8 \mu L$ of each primer (5 µM), 2 µL of 2.5 mM dNTPs, and 0.4 µL of FastPfu polymerase.

The Illumina 16S rRNA metagenomics sequencing library preparation procedure was used to create the 16S rRNA sequencing libraries (Illumina, San Diego, CA, USA). The AxyPrep Mag PCR Clean-up kit (AXYGEN, Big Flats, NY, USA) was used to clean the amplicon products after each PCR round during the library preparation process. Each time, the size of the amplicons was checked on a 1.5% agarose gel. For all 54 samples, Illumina sequencing libraries were created, and Quant-iT PicoGreen was used to determine the amplicon DNA concentration (Molecular Probes, Eugene, OR, USA). Equimolar amounts of the finished libraries were combined. Sequencing was performed on the Illumina MiSeq platform with v4 chemistry. Using the QIIME 1.9.0 program, the 16S rRNA gene amplicon sequence analysis was carried out. The QIIME reference sequence collection was used to cluster sequences with at least 97% identity into OTUs; any reads that missed the references were clustered from scratch. To prevent false positives that depend on the overall error rate of the sequencing process, OTUs with fewer than 50 reads were taken out of the dataset. As outliers, samples with fewer than 3600 sequences were also eliminated from the dataset. After filtering, the number of OTUs was adjusted to be the same as the sample with the fewest reads for the subsequent analysis.

Linear discriminant analysis effect size (LEfse) was used to identify the species with statistical differences between different groups, that is, biomarker species. Linear discriminant analysis (LDA) score is used to indicate the degree of influence of these species on the differences between groups. The higher the LDA score value, the greater the impact of the species on differences between groups. LEfse analysis was conducted by the "microeco" package using R v3.3.1. "All against all" was selected for multigroup comparison with LDA score > 2.5 and p < 0.05 filtering set.

Shannon Diversity was calculated using the software of Mothur v1.35.1. The data sets were tested for normality and homogeneity followed by one-way ANOVA to determine statistical significance. The non-parametric Kruskal–Wallis test

was used in place of the parametric test when at least one of the assumptions was broken. Post-hoc comparisons were carried out to determine the direction and amount of an effect when a significant difference between treatments was identified. LSD post hoc comparisons were used following an ANOVA, while Turkey post hoc was used following a Kruskal-Wallis test.

RNA extraction and transcriptome analysis

Three 100 mg samples of fresh *G. lemaneiformis* per treatment were taken on days 13 and 26. These samples were frozen in liquid nitrogen and stored at -80° C. The transcriptome data were analyzed following methods described by Jiang et al. (2022). FDR \leq 0.001 and the absolute value of \log_2 Fold Change \geq 1 were used to assess the significance of the change in gene expression across various treatment conditions, and *q*-values of 0.05 or higher were declared significantly enriched.

Statistical analysis

Results were expressed as means of three biological replicates \pm standard deviation. The SPSS v.26 was used for all data analysis except for that on bacterial diversity (see above). The variances were equal for all treatments, and the data were confirmed to have a normal distribution by the Shapiro–Wilk test (p > 0.05). Repeated measures ANOVA that is a three-factorial model was used to assess the effects of culture time, nitrogen and simulated heatwave on biomass, SGR, POC accumulation, net photosynthetic rate, dark respiration rate, PE, PC, DOC release rate, RDOC fraction, DOC accumulation, RDOC accumulation, bacterial abundance. A post hoc least significant difference test was used. For each test, a 95% confidence interval was established.

Results

Seaweed growth and biomass

SGR varied during 26 d of culture with nitrogen and simulated heatwave interacting with culture time (Fig. 1a; Table S1). By day 6, high nitrogen treatment combinations (HNHW⁻ and HNHW⁺) resulted in 40–61% increases in SGR, compared to the ambient nitrogen treatment combinations (ANHW⁻ and ANHW⁺) (Fig. 1a; Table S2). By day 13, high nitrogen increased SGR by 59% in non-heatwave flasks and by 98% in heatwave flasks (Table S2). From days 6 to 13, heatwave treatments led to larger decreases in SGR (29-45%) than no heatwave treatments (20-30%). Two-way ANOVA showed that heatwave and nitrogen had an interactive effect on SGR by day 19 (Table S2), with a 443% increase in growth under ambient nitrogen but a decrease of 71% under high nitrogen when exposed to the simulated heatwave. From days 19 to 26, SGR in the simulated heatwave remained stable, while it continued to decrease for high nitrogen-no heatwave flasks and increased for ambient nitrogen-no heatwave flasks. On day 26, SGRs converged with no significance differences among treatments.

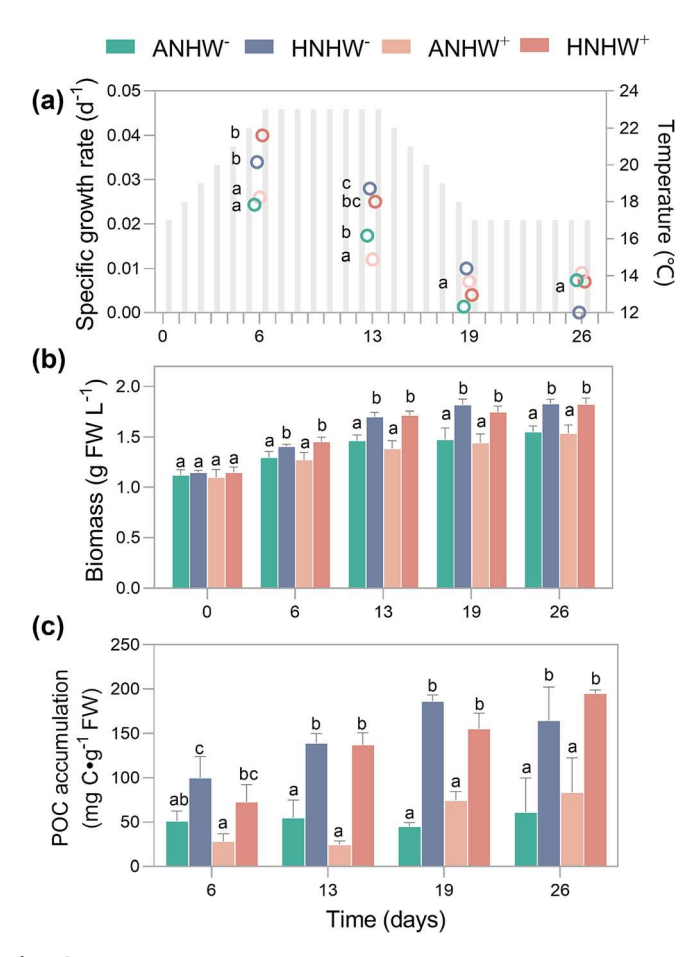


Fig. 1. SGR (**a**), biomass (**b**) and seaweed POC accumulation (**c**) of *G. lemaneiformis* over time in different treatment combinations. ANHW⁻, HNHW $^{-}$, ANHW $^{+}$, and HNHW $^{+}$, stand for ambient nitrogen-no heatwave, high nitrogen-no heatwave, ambient nitrogen with heatwave, and high nitrogen with heatwave conditions, respectively. Different letters indicate significant differences among the four treatment combinations (p < 0.05). Gray bars in panel a represent simulated heatwave temperatures, while all no-heatwave treatment combinations were maintained at 17° C throughout.

Culture time interacted with nitrogen on biomass of *G. lemaneiformis* (Fig. 1b; Table S1). Biomass had reached a plateau on day 19 for the high nutrient conditions whereas in the ambient nutrient conditions biomass was still building up in the cultures. At each time point, high nitrogen enhanced biomass while the simulated heatwave did not show significant effects (Table S2).

Regarding seaweed POC accumulation (Fig. 1c), culture time had an interactive effect with nitrogen or heatwave (Table S1). Heatwave and nitrogen both affected POC accumulation significantly after incubating for 6 d (Table S2). The simulated heatwave decreased it by 122% under ambient nitrogen condition and 32% under high nitrogen condition while high nitrogen showed a simulative effect. During the temperature maintaining period (days 6–13), nitrogen was

the only factor impacting the POC accumulation that was increased by 155% in non-heatwave conditions and by 460% in heatwave conditions. However, after the temperature decreased to the initial level (day 19), nitrogen and heatwave showed an interactive effect. High nitrogen increased POC accumulation by 3.44 times in non-heatwave conditions and by 1.16 times in heatwave conditions. At the end of experiment, high nitrogen increased seaweed POC accumulation by 1.43–1.80 times (Table S2).

Photosynthetic rates, respiration rates, and phycobiliproteins

Net photosynthetic rate of thalli varied depending on nitrogen levels throughout the incubations (Table S1; Fig. 2a). Net photosynthetic rate under high nitrogen conditions increased from days 0 to 6, then decreased till day 19 and increased a little by the end of a recovery period, while net photosynthetic rate under ambient nitrogen conditions did not show an increase from days 0 to 6 or during the recovery period. At the end of the temperature rising period (day 6), nitrogen affected net photosynthetic rate (Table S2) and high nitrogen increased it by 13-69% (Fig. 2a). After the high temperature maintained for 1 week (day 13), two-way ANOVA showed that heatwave and nitrogen had interactive effects on net photosynthetic rate (Table S2). High nitrogen increased net photosynthetic rate by 123% in non-heatwave conditions but did not affect it in heatwave conditions (Table S2). When temperature decreased to the initial temperature (day 19), the simulated heatwave showed a negative effect on net photosynthetic rate (Table S2) with the decrease of 54% under ambient nitrogen condition and 78% under high nitrogen condition. By the end of the experiment (day 26), two-way ANOVA showed an interactive effect of nitrogen and heatwave on net photosynthetic rate (Table S2). High nitrogen increased net photosynthetic rate by 152% under in non-heatwave conditions but did not affect it in heatwave conditions.

Dark respiration rate also varied with incubation and generally did not change or even increased a little during the heatwave stage but decreased during the recovery stage (Table S1; Fig. 2b). Neither nitrogen nor heatwave affected dark respiration rate on day 6 and high nitrogen increased it by 36–40% compared to ambient nitrogen on day 13 (Table S2). On day 19, the simulated heatwave decreased dark respiration rates by 22–29% (Table S2). All effects disappeared at the end of experiment (Table S2).

Changes in phycobilin protein levels in the four treatment combinations are shown in Fig. 2c,d and both PE and PC content decreased with culture time (Table S1). The simulated heatwave affected the PE content significantly on day 6 (Table S2) and decreased it by 24% in ambient nitrogen conditions and 9% in high nitrogen conditions (Fig. 2c). On day 13, high nitrogen significantly enhanced PE by 67–72%. On day 19, the simulated heatwave reduced PE by 36% in ambient nitrogen conditions but did not affect it in high nitrogen

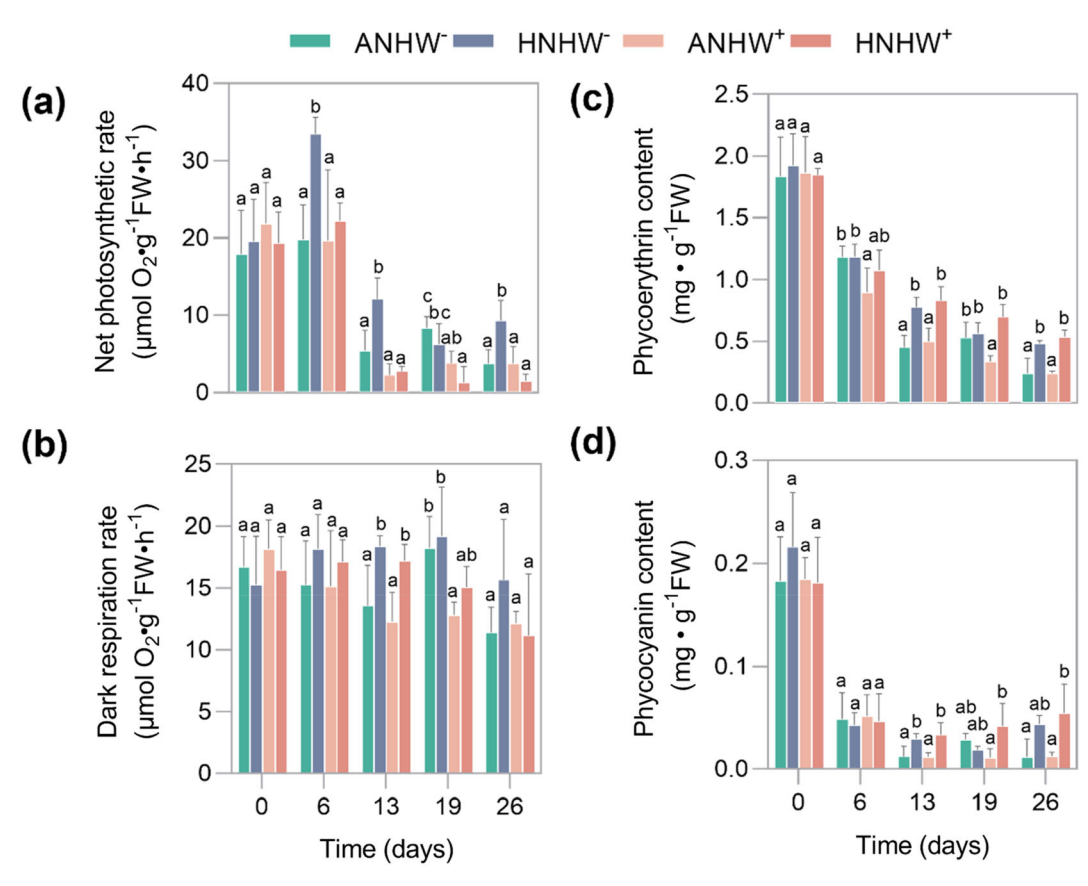


Fig. 2. Net photosynthetic rate (**a**), dark respiration rate (**b**), PE (**c**), and PC (**d**) levels of *G. lemaneiformis* in heatwave and nitrogen level treatments. ANHW⁻, HNHW⁻, ANHW⁺, and HNHW⁺, stand for ambient nitrogen-no heatwave, high nitrogen-no heatwave, ambient nitrogen with heatwave, and high nitrogen with heatwave conditions. Different letters indicate significant differences among four conditions (p < 0.05). Please see Fig. 1a for temperature change during the simulated heatwave while all no-heatwave treatment combinations were maintained at 17°C throughout.

conditions, showing an interactive effect with nitrogen. At the end of experiment (day 26), high nitrogen showed a large stimulating effect, enhancing PE by 102–123%. In terms of PC (Fig. 2d), no difference among treatments was found on day 6 while high nitrogen significantly increased PC by 143% under non-heatwave and 181% under heatwave on day 13 (Table S2; Fig. 2d). The simulated heatwave interacted with nitrogen on day 19, decreasing PC by 61% in ambient nitrogen conditions but increasing it by 124% under high nitrogen conditions (Table S2). By the end of the experiment, PC content of this commercially important seaweed was increased by high nitrogen by 268% in non-heatwave conditions and 333% in heatwave conditions.

DOC release by *G. lemaneiformis* and transformation by bacteria

There was an interactive effect of incubation time with heatwave on DOC release rate (Table S1; Fig. 3a). With no significant effects of heatwave or nitrogen on days 6 and 13, they interacted on DOC release rate on day 19 (Table S3). The simulated heatwave increased DOC release rate by almost 20 times

in ambient nitrogen conditions but did not affect it in high nitrogen conditions (Fig. 3a). On day 26, heatwave decreased the DOC release rate by 58% in ambient nitrogen conditions and 93% under high nitrogen conditions (Table S3).

High nitrogen decreased the RDOC fraction by 3.6% in non-heatwave conditions and 26% in heatwave conditions on day 66 but increased it by 56% under non-heatwave conditions and by 38% under heatwave conditions on day 73 (Fig. 3b; Table S3). On day 79, the simulated heatwave increased RDOC fraction by 30% under ambient nitrogen and 28% under high nitrogen (Table S3). On day 86, both the simulated heatwave and high nitrogen had negative effects, reducing RDOC fraction by 62-65% and 18-25% respectively. DOC and RDOC released at each time point were used to assess their accumulation (Fig. 3c,d). DOC accumulation increased with culture time but the patterns were different under various conditions with that under ambient nitrogen with heatwave having the largest increase (Table S1). During the first 13 d of culture, neither the simulated heatwave nor nitrogen affected DOC accumulation. However, the simulated heatwave increased DOC accumulation by 194% under

19395590, 0, Downloaded from https://aslopubs.onlinelibrary.wiley.com/doi/10.1002/lno.12487 by Plymouth University, Wiley Online Library on [02/01/2024]. See the Terms

and-conditions) on Wiley Online Library for rules of use; OA articles are governed by the applicable Creative Commons Licenso

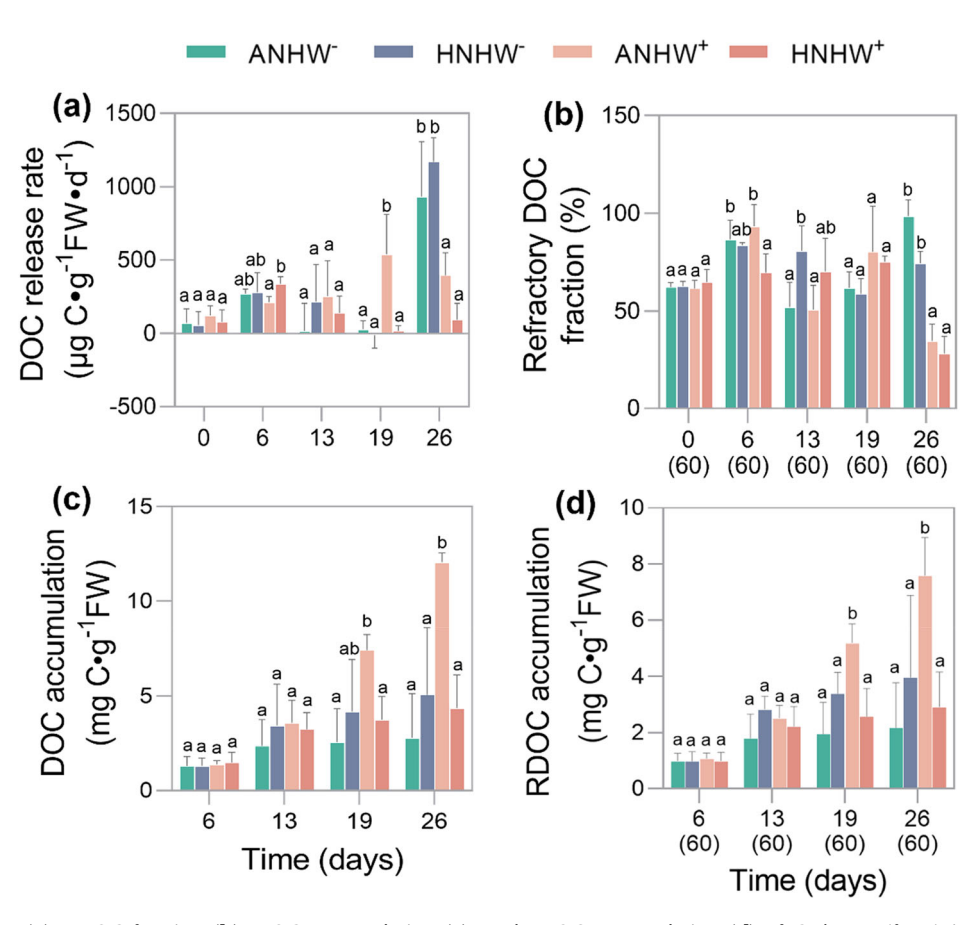


Fig. 3. DOC release rate (**a**), RDOC fraction (**b**), DOC accumulation (**c**), and RDOC accumulation (**d**) of *G. lemaneiformis* in each heatwave/nitrogen treatment. ANHW $^-$, HNHW $^-$, ANHW $^+$, and HNHW $^+$, stand for ambient nitrogen-no heatwave, high nitrogen-no heatwave, ambient nitrogen with heatwave, and high nitrogen with heatwave. The (60) in panels b and d represents the samples collected on days 0, 6, 13, 19, and 26 being incubated for 60 d. Different letters indicate significant differences among four treatment combinations (p < 0.05). Please see Fig. 1a for temperature change during the simulated heatwave while all no-heatwave treatment combinations were maintained at 17 $^{\circ}$ C throughout.

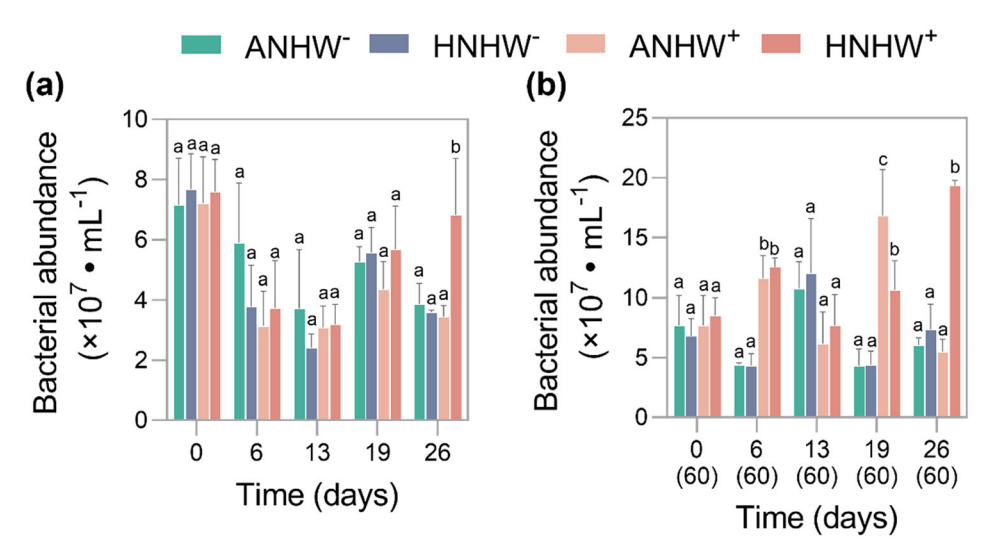


Fig. 4. Bacterial abundance in different heatwave and nitrogen treatments. (**a**) Bacterial abundance during seaweed incubation period, (**b**) bacterial abundance after 2-month of dark incubation. ANHW $^-$, HNHW $^-$, ANHW $^+$, and HNHW $^+$, stand for ambient nitrogen-no heatwave, high nitrogen-no heatwave, ambient nitrogen with heatwave, and high nitrogen with heatwave conditions. The (60) in panel b represents the samples collected on days 0, 6, 13, 19 and 26 being incubated for 60 d. Different letters indicate significant differences among four treatment combinations (p < 0.05). Please see Fig. 1a for temperature change during the simulated heatwave while all no-heatwave treatment combinations were maintained at 17 $^{\circ}$ C throughout.

ambient nitrogen conditions while did not affect it under high nitrogen conditions by day 19 (Fig. 3c; Table S3). At the end of the 26-day incubation period, the simulated heatwave also interacted with nitrogen, increasing DOC accumulation by 333% under ambient nitrogen conditions while with no significant effect under high nitrogen conditions. RDOC accumulation also increased with culture time with that under ambient nitrogen with heatwave conditions having the largest increase (Table S1; Fig. 3d). There was no significant difference of RDOC accumulation among treatment combinations during the first 73 d of incubation. By day 79, the interactive effect of heatwave and nitrogen occurred (Table S3); the simulated heatwave enhanced RDOC accumulation by 166% under

ambient nitrogen but did not significantly affect it under high nitrogen (Fig. 3d; Table S3). At the end of incubation, similar to day 79, the simulated heatwave increased RDOC accumulation by 249% under ambient nitrogen conditions but did not significantly affect it under high nitrogen conditions (Fig. 3d; Table S3).

Bacterial abundance in differing heatwave and nitrogen conditions

Bacterial abundance fluctuated with culture time (Table S1; Fig. 4a). Heatwave and nitrogen did not affect it by day 19, but they had an interactive effect on day 26 (Table S3). The simulated heatwave did not affect bacterial abundance at

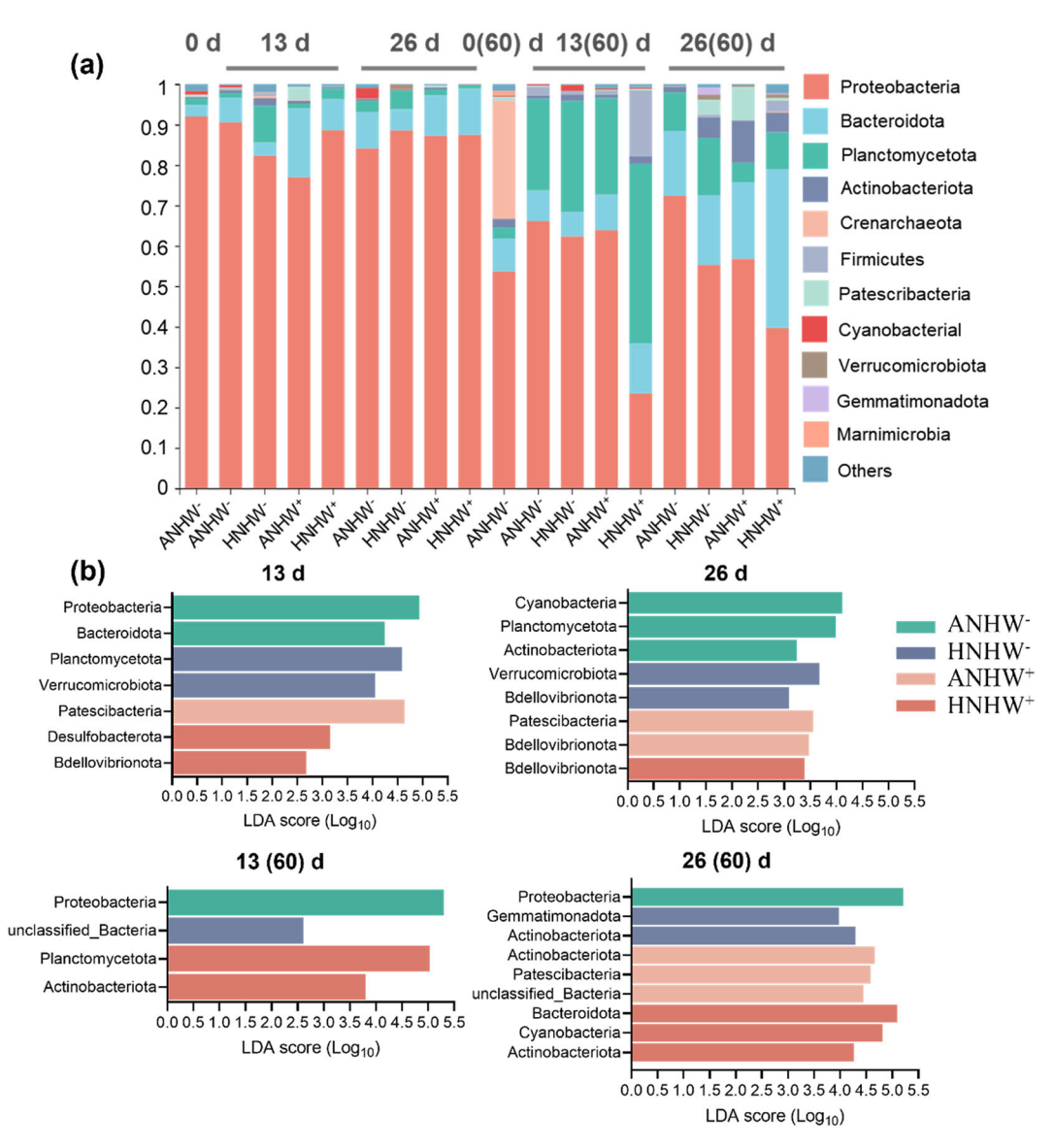


Fig. 5. Relative abundance of dominant bacterial phyla (contributing more than 1% to the total bacterial community) (**a**) and LDA score (**b**) on different days. ANHW⁻, HNHW⁻, ANHW⁺ and HNHW⁺, stand for ambient nitrogen-no heatwave, high nitrogen-no heatwave, ambient nitrogen with heatwave, high nitrogen with heatwave conditions, respectively. The (60) represents the samples collected on days 0, 13, and 26 being incubated for 60 d. Please see Fig. 1a for temperature change during the simulated heatwave while all no-heatwave treatment combinations were maintained at 17°C throughout.

ambient nitrogen levels but increased it by 162% at high nitrogen levels (Fig. 4a). The simulated heatwave decreased the bacterial abundance by 11%, though the difference was insignificant. As for bacterial abundance after 2 months in the dark, there were interactive effects of time, nitrogen and heatwave (Table S1); bacterial abundance in non-heatwave conditions did not change, while it decreased in ambient nitrogen with heatwave conditions and increased under high nitrogen with heatwave (Fig. 4b). The heatwave simulations influenced the bacterial abundance significantly from days 66 to 79 (Table S3), which increased it on days 66 and 79, while decreased it on day 73 (Fig. 4b). At the end of the experiment, heatwave and nitrogen interacted on the bacterial abundance (Table S3). The simulated heatwave enhanced the bacterial abundance by 162% at high nitrogen but did not affect it at ambient nitrogen.

Phycosphere bacteria in different N and heatwave conditions

Gracilaria lemaneiformis bacterial communities were monitored in four treatment combinations (Fig. 5). 16S rRNA gene sequencing from 54 colonies of the culture medium, yielded 447,168 sequences that were further clustered into 3992 OTUs. Samples associated with 48 unique bacterial phyla, 120 classes, and 299 orders. The most abundant phylum across all samples under various treatments was Proteobacteria (23–92%), followed by Bacteroidota (4–40%), and Planctomycetota (1–45%) (Fig. 5a).

The LEfse analysis was used to detect signature species that significantly changed in phycosphere bacteria of *G. lemaneiformis* under various nitrogen and heatwave conditions (Fig. 5b). Comparing the specific groups of bacteria under different treatments, it was found that on day 13,

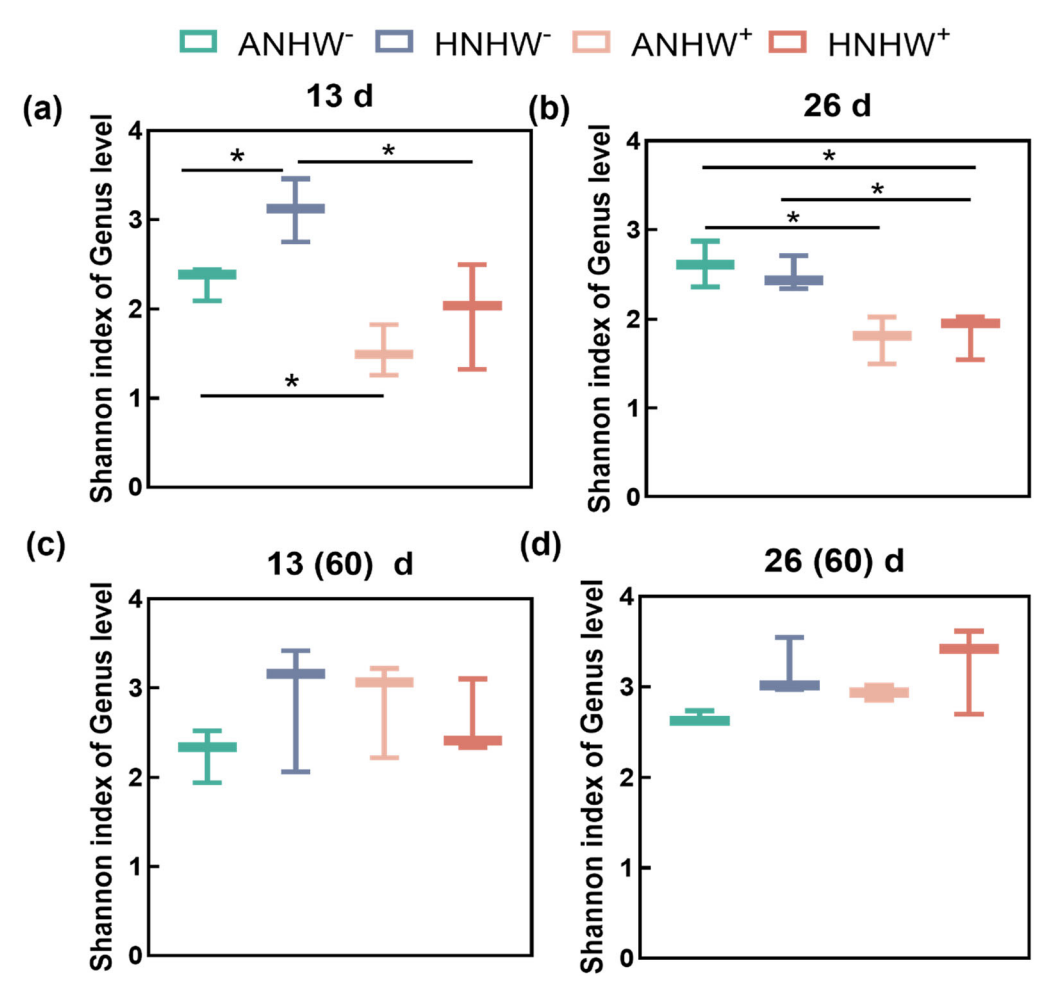


Fig. 6. Shannon diversity of bacterial genera living on cultured *Gracilaria* under each treatment on different days. ANHW⁻, HNHW⁻, ANHW⁺, and HNHW⁺, stand for ambient nitrogen-no heatwave, high nitrogen-no heatwave, ambient nitrogen with heatwave, high nitrogen with heatwave conditions, respectively. The (60) in panels (**c**) and (**d**) represents the samples collected on days 13 and 26 being incubated for 60 d. Both ends of the horizontal line are the two sides of the comparison. The *p*-value (*p*) indicates the significance of the differences based on a Kruskal–Wallis test with * means $0.01 . Please see Fig. 1a for temperature change during the simulated heatwave while all no-heatwave treatment combinations were maintained at <math>17^{\circ}$ C throughout.

Proteobacteria, Planctomycetota, Patescibacteria, and Desulfobacterota were significantly enriched under the conditions of ambient nitrogen-no heatwave, high nitrogen-no heatwave, ambient nitrogen with heatwave, and high nitrogen with heatwave, respectively. On day 26, Cyanobacteria Planctomycetota were significantly enriched under ambient nitrogen-no heatwave, Verrucomicrobiota and Bdellovibrionota were significantly enriched under high nitrogen-no heatwave, Patescibacteria and Bdellovibrionota were significantly enriched under ambient nitrogen with heatwave, and Bdellovibrionota were significantly enriched under high nitrogen with heatwave. On day 73, Proteobacteria, one unclassified bacterial and Planctomycetota were significantly enriched under ambient nitrogen-no heatwave, high nitrogen-no heatwave, and high nitrogen with heatwave, respectively. On day 86, Proteobacteria, Gemmatimonadota were significantly enriched under ambient nitrogen-no heatwave and high nitrogen-no heatwave, respectively. Actinobacteriota and Patescibacteria were significantly enriched under ambient nitrogen with heatwave. Bacteroidota and Cyanobacteria were enriched under high nitrogen with heatwave.

Comparisons between experimental culture conditions revealed significant differences in α diversity (Fig. 6). On day 13 (Fig. 6a), high nitrogen increased the Shannon index by 35% while the simulated heatwave had a negative effect, resulting in a neutral result when they both combined. On day 26 (Fig. 6b), the simulated heatwave decreased the Shannon index by 32% in ambient nitrogen conditions and by 26% in high nitrogen conditions (p < 0.05). The combination of heatwave and high nitrogen decreased the Shannon index by 30% (p < 0.05). After 2 months of dark incubation (days 73 and 86), the alpha diversity of all

treatments converged and did not differ significantly (Fig. 6c,d, p > 0.05).

Transcriptomic responses of G. lemaneiformis on day 13

Differential expression of genes exhibited the influences of nitrogen and a simulated heatwave on G. lemaneiformis at the molecular level (Fig. 7). The *t*-tests with q-value < 0.05 revealed 4929 differential expression genes between ambient nitrogenno heatwave and ambient nitrogen with heatwave conditions, 2430 differential expression genes between ambient nitrogenno heatwave and high nitrogen-no heatwave conditions, and 8936 differential expression genes between ambient nitrogenno heatwave and high nitrogen with heatwave conditions on day 13 (Fig. 7a). Therefore, the simulated heatwave has a stronger effect on G. lemaneiformis than nitrogen in terms of the number of differential expression genes, and the combined effects of nitrogen and heatwave caused more changes than nitrogen or heatwave individually. However, only the simulated heatwave had significant effects (q-value < 0.05) on day 13 based on KEGG (Kyoto Encyclopedia of Genes and Genomes) pathway enrichment analysis. Base excision repair and nucleotide excision repair were significantly changed KEGG pathways (Fig. 7b). Genes related to base excision repair (AlkA, UNG, PCNA, Dpol, Xth, Pok, and PARP) were significantly down-regulated by 0.8-3.65 log₂ folds and genes of nucleotide excision repair (RBX1, DDB1, DDB2, XPC, HR23B, CDK7, MNAT1, TFllH1, XPG, RPA, PCNA, and RFC) were significantly down-regulated by 0.36-4.07 log₂ folds. Glycerolipid metabolism was also a noticeable KEGG pathway in which the genes such as glpK, AGPAT9, plsC, LPIN, ATG15, and PPIB were upregulated by 1.28–2.42 log₂ folds (Fig. 7c).

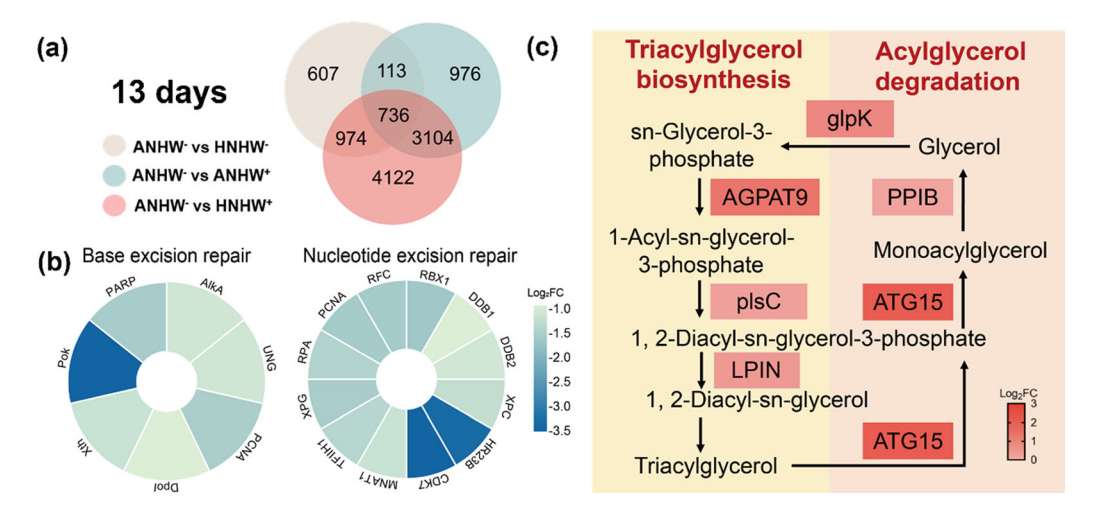


Fig. 7. Differential expression genes and KEGG pathways in *G. lemaneiformis* on day 13. (a) Venn diagram of the number of shared or unique *G. lemaneiformis* differential expression genes under ANHW⁻ vs. HNHW⁻, ANHW⁻ vs. ANHW⁺, and ANHW⁻ vs. HNHW⁺. (b) Heatmap of genes related to base excision repair and nucleotide excision repair by heatwaves (ANHW⁻ vs. ANHW⁺). (c) Changes in expression of genes associated with glycerolipid metabolism by heatwaves (ANHW⁻ vs. ANHW⁺). ANHW⁻, ANHW⁺, and HNHW⁺, stand for ambient nitrogen-no heatwave, high nitrogen-no heatwave, ambient nitrogen with heatwave, high nitrogen with heatwave conditions, respectively. The color represents the difference in log₂fold. Please see Fig. 1a for temperature change during the simulated heatwave while all no-heatwave treatment combinations were maintained at 17°C throughout.

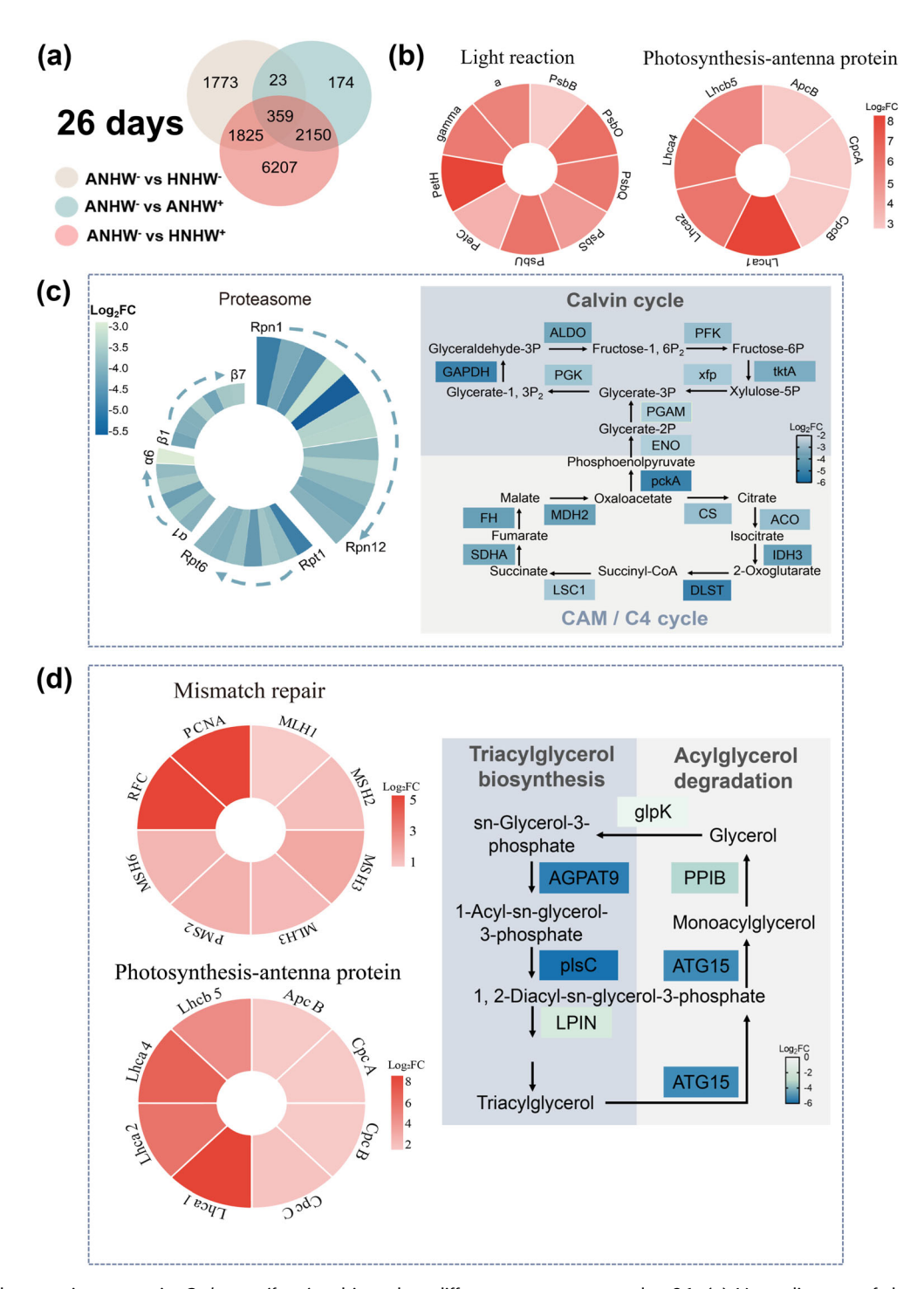


Fig. 8. Differential expression genes in *G. lemaneiformis* subjected to different treatments on day 26. (**a**) Venn diagram of the number of shared or unique *G. lemaneiformis* differential expression genes under ANHW⁻ vs. HNHW⁻, ANHW⁻ vs. ANHW⁺, and ANHW⁻ vs. HNHW⁺ on day 26. (**b**) Heatmap of genes related to photosynthesis-light reaction and photosynthesis-antenna protein under ANHW⁻ vs. HNHW⁻. (**c**) Heatmap of genes related to proteasome and changes in expression of genes associated with carbon metabolism (Calvin cycle and CAM/C4 cycle) under ANHW⁻ vs. ANHW⁺. (**d**) Heatmap of genes related to photosynthesis-antenna protein and mismatch repair, changes in expression of genes associated with glycerolipid metabolism (triacylglycerol biosynthesis and acylglycerol degradation) under ANHW⁻ vs. HNHW⁺. ANHW⁻, HNHW⁻, ANHW⁺, and HNHW⁺, stand for ambient nitrogen-no heatwave, high nitrogen-no heatwave, ambient nitrogen with heatwave, high nitrogen with heatwave conditions, respectively. The color represents the difference in log₂fold. Please see Fig. 1a for temperature change during the simulated heatwave while all no-heatwave treatment combinations were maintained at 17°C throughout.

Jiang et al.

Transcriptomic responses of G. lemaneiformis on day 26

Comparisons between treatments revealed 2706 differential expression genes between ambient nitrogen-no heatwave and ambient nitrogen with heatwave conditions, 3980 differential expression genes between ambient nitrogen-no heatwave and high nitrogen-no heatwave conditions, and 10,541 differential expression genes between ambient nitrogen-no heatwave and high nitrogen with heatwave conditions on day 26 (Fig. 8a). Therefore, at the end of the experiment, nitrogen had larger effects on *G. lemaneiformis* compared to the simulated heatwave.

Genes related to photosynthesis-light reaction (PsbB, PsbO, PsbQ, PsbS, PsbU, PetC, PetH, gamma, and α) and photosynthesisantenna protein (ApcB, CpcA, CpcB, Lhca1, Lhca2, Lhca4, and Lhcb5) were upregulated significantly by high nitrogen (ANHWvs. HNHW⁻) on day 26 (Fig. 8b). While the simulated heatwave revealed the negative effects mainly on proteasome and carbon metabolism (Fig. 8c), downregulating genes related to proteasome (*Rpn1-Rpn12*, *Rpt1-Rpt6*, $\alpha 1-\alpha 6$, and $\beta 1-\beta 7$) by 2.74– 5.76 log₂folds (ANHW⁻ vs. ANHW⁺). Two pathways of carbon metabolism, the Calvin cycle and the CAM/C4 cycle, were both affected by heatwave treatments. Genes related to the Calvin cycle (ALDO, GAPDH, PGK, PFK, xfp, tktA, PGAM, and ENO) were downregulated by 3.05-5.19 log₂ folds and that related to CAM/C4 cycle were downregulated by 3.2-5.21 log₂ folds. Three pathways were significantly altered in response to the combined effects of nitrogen and a simulated heatwave (Fig. 8d). Genes related to photosynthesis-antenna protein (ApcB, CpcA, CpcB, CpcC, Lhca1, Lhca2, Lhca4, and Lhcb5) were upregulated significantly by 1.04-8.71 log₂ folds. Meanwhile, genes related to mismatch repair (MLH1, MSH2, MSH3, MLH3, PMS2, MSH6, RFC, PCNA, and Polδ) were also upregulated significantly by 0.58-5.28 log₂ folds. On the other hand, genes related to glycerolipid metabolism (glpK, AGPAT9, plsC, LPIN, ATG15, and PPIB) were downregulated by 1.12-5.97 log₂ folds.

Discussion

This study differs from the usual types of laboratory experiments that are designed to investigate the effects of different but steady temperatures to test the effects of climate change on organisms. Here, we simulated a realistic marine heatwave event using a 6-day period of warming, a week of high seawater temperature and then a cooling period back down to seasonally normal temperatures.

Simulated heatwave and nitrogen affect growth, photosynthesis, and seaweed POC production

Seaweed growth determines their particle organic carbon production (Sambhwani et al. 2022). Here, simulated heatwave conditions initially stimulated growth of the commercially important seaweed *G. lemaneiformis* but then negatively affected growth. After 26 d of culture, the effect of simulated heatwave on biomass and POC production was

neutral. Therefore, the effects of heatwave depend on their intensity and duration (Saha et al. 2020). Temperature increases can benefit aquaculture seaweeds but only if within their thermal tolerance window (Egea et al. 2022). For instance, a seawater temperature rise from 20°C to 24°C can enhance growth of G. lemaneiformis (Liu et al. 2018) but an increase from 25°C to 30°C reduces its growth (Wang et al. 2016). We demonstrate that a realistic simulated heatwave event can damage photosynthesis and growth of G. lemaneiformis. Transcriptomic data show that the simulated heatwave downregulated genes related to proteasome, base and nucleotide excision repair, and the Calvin cycle. Proteasomes are protein complexes which degrade unneeded or damaged proteins by proteolysis. The proteasomal degradation pathway is essential for many cellular processes, including the cell cycle, the regulation of gene expression, and responses to oxidative stress (Collins and Goldberg 2017). Base and nucleotide excision repair is responsible for the recognition and repair of DNA damage caused by stressors such as ultra violet radiation and high temperatures. Down-regulation of these pathways reduces the ability of algae to repair the damage of heatwaves to photosynthetic carbon fixation.

Unlike the simulated heatwave, high nitrogen enhanced growth, biomass and POC accumulation of G. lemaneiformis. This is consistent with previous research where growth rate of G. lemaneiformis increased with nitrogen (from 10 to 367 µM) (Ma et al. 2021). The positive effect of increased nitrogen on growth is related to photosynthesis since in our study high nitrogen levels increased phycobilin pigment contents and photosynthetic rates. Transcriptomic data show that high levels of nutrients upregulated gene expression of photosynthesis-light reaction and photosynthesis-antenna proteins. Meanwhile, physiological performances of G. lemaneiformis cultured under all conditions, including SGR, net photosynthesis rate, the content of PE, PC, and nitrogen, decreased after day 13. This is usual for both laboratory and field culture of G. lemaneiformis due to increased biomass and decreased available light (Yang et al. 2006; Yu and Yang 2008; Duan et al. 2019). Our nutrient data show nitrogen levels were high under high nitrogen conditions during the culture period (Fig. S1). A possible explanation for intermittent periods of nitrogen limitation around thalli under high nitrogen conditions is increased biomass density and limited water motion between water changes and stirring events. However, we consider these effects were minor because both biomass and nitrogen content under high nitrogen conditions were significantly higher than those under ambient nitrogen conditions. For this aquaculture species high nitrogen could help it withstand heatwave episodes. For instance, the simulated heatwave reduced the content of PE and PC under ambient nitrogen on day 19 but did not affect them under high nitrogen. Gene expression of photosynthesisantenna protein and mismatch repair was also upregulated under the combination of high nitrogen and heatwave.

DOC production and transformation in various conditions

Production, consumption and transformation of DOC are essential parts of the marine carbon cycle. Seaweeds release large quantities of DOC and some of this is transformed into RDOC by bacteria (Wada et al. 2008). We found that the simulated heatwave stimulated DOC release during the high temperature and subsequent cooling periods, resulting in increased DOC release over the 26 d experiment. This is consistent with reported effects in microalgae. For instance, DOC production increased with temperature for Chlorella vulgaris (5–20°C) and Synechococcus sp. (5–30°C) (Zlotnik and Dubinsky 1989). The stimulative effect of high temperature on DOC release could be attributed to the change of the mobility of cell membrane molecules. High temperatures can enhance the rate of transmembrane transport of substances and thus DOC release (Myklestad and Swift 1998; Gao et al. 2021c). In addition, genes related to base and nucleotide excision repair and proteasome were significantly downregulated in G. lemaneiformis under simulated heatwave conditions. Base and nucleotide excision repair has shown their crucial roles in maintaining genomic integrity particularly in response to exposure to ultraviolet light and reactive oxygen species (Connelly et al. 2009; Izumi and Mellon 2021). Proteasomes allow cells to regulate protein concentrations. This is essential for many cellular processes, including the cell cycle, the regulation of gene expression, and responses to oxidative stress (Xu and Xue 2019). When proteasome repair mechanisms are compromised, algal physiology and membrane function can be damaged, leading to the increase in membrane permeability and DOC release. In addition, simulated heatwave led to the enrichment of Bdellovibrionota and Patescibacteria in this study. Bacteria in Bdellovibrionota, e.g., Bdellovibrio, prey upon other larger gram-negative bacteria (Sockett 2009), which can reduce bacteria abundance and thus DOC consumption. Due to the loss of some key metabolic genes, the capacity of Patescibacteria in utilizing DOC may be restricted (Lemos et al. 2019). Therefore, the data of bacteria also support the increased DOC production in simulated heatwave conditions.

When *G. lemaneiformis* was grown under high nitrogen conditions, the loss of DOC in simulated heatwave conditions were largely neutralized. It seems that by enhancing photosynthesis and cell repair gene functions, *G. lemaneiformis* was able to counteract heatwave damage and protect the ability of its cell membranes to retain fixed carbon. As expected, high nutrients increased nitrogen content of thalli and these individuals did not need to excrete DOC to maintain a stable C/N ratio (Fig. S2). High nitrogen levels combined with the simulated heatwave conditions resulted in increased bacterial abundance on day 26, which also contributed to decreased DOC in the culture media since much of the DOC released by seaweeds could be degraded by phycosphere bacteria (Zhao et al. 2019).

Here, simulated heatwave conditions led to lower proportions of RDOC, which could be attributed to an enhanced

ability of bacteria to decompose DOC under higher temperatures. This result is consistent with field findings, in which warmer and darker seawater environments led to a decrease in the DOM inventory through enhanced microbial mineralization (Wang et al. 2021). This is related to the degradation of some semi-refractory components by bacteria at higher temperatures. In addition, a lower RDOC fraction during simulated heatwave conditions may result from excretion of more labile DOC, since high temperatures can affect the biochemical composition of G. lemaneiformis (Ma et al. 2021). Although simulated heatwave conditions enhanced microbial mineralization and led to lower fraction of RDOC, they also promoted the total release of DOC. Therefore, the amount of RDOC produced by G. lemaneiformis during 26 d of culture was increased by simulated heatwave conditions. This finding indicates that heatwaves could enhance the carbon sequestration by G. lemaneiformis while nitrogen enrichment can counteract this effect, although of course this would only be true in the real world if the seaweeds were able to survive the heatwave effect.

Effects of simulated heatwave and nitrogen on bacterial abundance and diversity

After 26 d of culture, bacterial abundance in high nitrogen with heatwave conditions was largely increased compared to the control, while individual high nitrogen or heatwave did not have any effect. A similar pattern was found for bacterial abundance after 2-month dark incubation. It seems that heatwave could only stimulate bacterial growth when nutrients are enough. Previous studies also showed the importance of nitrogen in supporting bacterial proliferation (Wang et al. 2022). After 26 d of incubation, simulated heatwave conditions significantly reduced bacterial diversity regardless of nitrogen concentration. High temperatures can generate some winners and losers, decreasing bacterial diversity (Minich et al. 2018). In the present study, Patescibacteria and Bdellovibrionota were significantly enriched in ambient nitrogen with heatwave conditions, and Bdellovibrionota was significantly enriched under high nitrogen with heatwave, indicating that these bacteria may become winners after exposure to heatwave. After 60 d of dark incubation, the effects of simulated heatwave on the Shannon index under various treatments converged, suggesting the disappearance of heatwave' effect on bacterial diversity. However, bacterial structure varied. Actinobacteriota and Patescibacteria were significantly enriched in ambient nitrogen with heatwave conditions, and Bacteroidota and Cyanobacteria were enriched in high nitrogen with heatwave conditions. The effects of heatwaves on bacterial structure may be related to DOC composition. A wider diversity of different DOC compounds can allow more diverse bacterial communities to develop (Chen et al. 2020). Therefore, heatwaves may change bacterial structure through affecting DOC composition excreted by seaweeds; a hypothesis requires testing in future studies.

Conclusion

Marine heatwaves are becoming more frequent, intense, and prolonged worldwide with seaweed cultivation seen as a potential way of removing and sequestering atmospheric carbon dioxide. This study is the first to investigate the combined effects of nitrogen and a simulated marine heatwave on carbon sequestration and phycosphere bacteria of seaweeds. Using a commonly cultivated macroalga, G. lemaneiformis, we found that a simulated marine heatwave caused significant increases in DOC and RDOC production at the levels of nitrogen found around Chinese aquaculture facilities accompanied by a decreased diversity of bacteria living on the seaweeds and an increase in heterotrophic bacteria. When nitrogen conditions were increased even higher than this, then DOC release by the seaweeds was reduced. This suggests that the economic seaweed G. lemaneiformis would lose substantial amounts of DOC and RDOC into nearshore waters during marine heatwaves unless their growth and photosynthesis were supported by high levels of nitrogen availability. Given that eutrophication is already a stressor along Chinese coasts, this should not be seen as a solution to combatting the effect of marine heatwaves on seaweed aquaculture facilities. More studies should be conducted to investigate the combined effects of marine heatwaves and nutrients on the carbon sequestration of other seaweeds and the carbon cycle in coastal ecosystems since these two stressors are on the increase worldwide. It is also recommended to conduct field experiments during real marine heatwave events to test the conclusions drawn from simulated experiments.

Data availability statement

Data available via the Dryad Digital Repository https://datadryad.org/stash/share/A6Gu7J76X6UL21RnrO_Dk-eR4paQbn TPjZvD-ACD75s.

References

- Agostini, S., and others. 2021. Simplification, not "tropicalization", of temperate marine ecosystems under ocean warming and acidification. Glob. Chang. Biol. **27**: 4771–4784. doi:10.1111/gcb.15749
- Beer, S., and A. Eshel. 1985. Determining phycoerythrin and phycocyanin concentrations in aqueous crude extracts of red algae. Aust. J. Mar. Fresh. Res. **36**: 785–792. doi:10. 1071/MF9850785
- Brauko, K. M., and others. 2020. Marine heatwaves, sewage and eutrophication combine to trigger deoxygenation and biodiversity loss: A SW Atlantic case study. Front. Mar. Sci. **7**: 590258. doi:10.3389/fmars.2020.590258
- Chen, J. H., M. Li, Z. H. Zhang, C. He, Q. Shi, N. Z. Jiao, and Y. Y. Zhang. 2020. DOC dynamics and bacterial community succession during long-term degradation of *Ulva prolifera* and their implications for the legacy effect of green

- tides on refractory DOC pool in seawater. Water Res. **185**: 116268. doi:10.1016/j.watres.2020.116268
- Collins, G. A., and A. L. Goldberg. 2017. The logic of the 26S proteasome. Cell **169**: 792–806.
- Connelly, S. J., R. E. Moeller, G. Sanchez, and D. L. Mitchell. 2009. Temperature effects on survival and DNA repair in four freshwater cladoceran *daphnia* species exposed to UV radiation. Photochem. Photobiol. **85**: 144–152. doi:10. 1111/j.1751-1097.2008.00408.x
- Duan, Y., N. Yang, M. Hu, Z. Wei, H. Bi, Y. Huo, and P. He. 2019. Growth and nutrient uptake of *Gracilaria lemaneiformis* under different nutrient conditions with implications for ecosystem services: A case study in the laboratory and in an enclosed mariculture area in the East China Sea. Aquat. Bot. **153**: 73–80.
- Egea, L. G., and others. 2022. Effect of marine heat waves on carbon metabolism, optical characterization, and bioavailability of dissolved organic carbon in coastal vegetated communities. Limnol. Oceanogr. **68**: 467–482.
- Feng, Y., and others. 2023. Shift in algal blooms from microto macroalgae around China with increasing eutrophication and climate change. Glob. Chang. Biol. **30**: e17018. doi:10.1111/gcb.17018
- Fernandez, P. A., J. D. Gaitan-Espitia, P. P. Leal, M. Schmid, A. T. Revill, and C. L. Hurd. 2020. Nitrogen sufficiency enhances thermal tolerance in habitat-forming kelp: Implications for acclimation under thermal stress. Sci. Rep. **10**: 3186. doi:10.1038/s41598-020-60104-4
- Follett, C. L., D. J. Repeta, D. H. Rothman, L. Xu, and C. Santinelli. 2014. Hidden cycle of dissolved organic carbon in the deep ocean. Proc. Natl. Acad. Sci. USA 111: 16706–16711.
- Gao, G., A. S. Clare, C. Rose, and G. S. Caldwell. 2018. *Ulva rigida* in the future ocean: Potential for carbon capture, bioremediation and biomethane production. GCB Bioenergy **10**: 39–51. doi:10.1111/gcbb.12465
- Gao, G., L. Gao, M. J. Jiang, A. Jian, and L. W. He. 2021a. The potential of seaweed cultivation to achieve carbon neutrality and mitigate deoxygenation and eutrophication. Environ. Res. Lett. **17**: 014018. doi:10.1088/1748-9326/ac3fd9
- Gao, G., X. Zhao, M. J. Jiang, and L. Gao. 2021*b*. Impacts of marine heatwaves on algal structure and carbon sequestration in conjunction with ocean warming and acidification. Front. Mar. Sci. **8**: 758651.
- Gao, G., J. Beardall, P. Jin, L. Gao, S. Xie, and K. Gao. 2022. A review of existing and potential blue carbon contributions to climate change mitigation in the Anthropocene. J. Appl. Ecol. **59**: 1686–1699. doi:10.1111/1365-2664.14173
- Gao, Y. P., and others. 2021c. Dissolved organic carbon from cultured kelp *Saccharina japonica*: Production, bioavailability, and bacterial degradation rates. Aquacult. Env. Interact. **13**: 101–110. doi:10.3354/AEI00393
- Gouvea, L. P., and others. 2017. Interactive effects of marine heatwaves and eutrophication on the ecophysiology of a

- widespread and ecologically important macroalga. Limnol. Oceanogr. **62**: 2056–2075. doi:10.1002/lno.10551
- Hobday, A. J., and others. 2016. A hierarchical approach to defining marine heatwaves. Prog. Oceanogr. **141**: 227–238. doi:10.1016/j.pocean.2015.12.014
- Hong, H., and others. 2017. The complex effects of ocean acidification on the prominent N_2 -fixing cyanobacterium *Trichodesmium*. Science **356**: 527–531. doi:10.1126/science. aal2981
- Izumi, T., and I. Mellon. 2021. Base excision repair and nucleotide excision repair, p. 293–322. *In* I. Kovalchuk and O. Kovalchuk [eds.], Genome stability. Academic Press.
- Jiang, M., L. Gao, R. Huang, X. Lin, and G. Gao. 2022. Differential responses of bloom-forming *Ulva intestinalis* and economically important *Gracilariopsis lemaneiformis* to marine heatwaves under changing nitrate conditions. Sci. Total Environ. 840: 156591. doi:10.1016/j.scitotenv.2022. 156591
- Jiao, N. Z., and others. 2010. Microbial production of recalcitrant dissolved organic matter: Long-term carbon storage in the global ocean. Nat. Rev. Microbiol. **8**: 593–599. doi:10. 1038/nrmicro2386
- Lemos, L. N., J. D. Medeiros, F. Dini-Andreote, G. R. Fernandes, A. M. Varani, G. Oliveira, and V. S. Pylro. 2019. Genomic signatures and co-occurrence patterns of the ultra-small Saccharimonadia (phylum CPR/Patescibacteria) suggest a symbiotic lifestyle. Mol. Ecol. **28**: 4259–4271.
- Li, Y., G. Y. Ren, Q. Y. Wang, and Q. L. You. 2019. More extreme marine heatwaves in the China seas during the global warming hiatus. Environ. Res. Lett. **14**: 104010. doi: 10.1088/1748-9326/ab28bc
- Liu, L., D. Zou, H. Jiang, B. Chen, and X. Zeng. 2018. Effects of increased CO_2 and temperature on the growth and photosynthesis in the marine macroalga *Gracilaria lemaneiformis* from the coastal waters of South China. J. Appl. Phycol. **30**: 1271–1280.
- Ma, C., S. Qin, H. L. Cui, Z. Y. Liu, L. C. Zhuang, Y. Wang, and Z. H. Zhong. 2021. Nitrogen enrichment mediates the effects of high temperature on the growth, photosynthesis, and biochemical constituents of *Gracilaria blodgettii* and *Gracilaria lemaneiformis*. Environ. Sci. Pollut. Res. 28: 21256–21265. doi:10.1007/s11356-020-11969-5
- Mantri, V. A., and others. 2022. Overview of global Gracilaria production, the role of biosecurity policies and regulations in the sustainable development of this industry. Rev. Aquacult. **15**: 801–819.
- Meinita, M. D. N., B. Marhaeni, Y. K. Hong, and G. T. Jeong. 2017. Enzymatic saccharification of agar waste from *Gracilaria verrucosa* and *Gelidium latifolium* for bioethanol production. J. Appl. Phycol. **29**: 3201–3209. doi:10.1007/s10811-017-1205-4
- Minich, J. J., M. M. Morris, M. Brown, M. Doane, M. S. Edwards, T. P. Michael, and E. A. Dinsdale. 2018. Elevated temperature drives kelp microbiome dysbiosis, while

- elevated carbon dioxide induces water microbiome disruption. PloS One **13**: e0192772. doi:10.1371/journal.pone. 0192772
- Myklestad, S. M., and E. Swift. 1998. A new method for measuring soluble cellular organic content and a membrane property, T_m, of planktonic algae. Eur. J. Phycol. **33**: 333–336. doi:10.1080/09670269810001736823
- Nepper-Davidsen, J., D. T. Andersen, and M. F. Pedersen. 2019. Exposure to simulated heatwave scenarios causes long-term reductions in performance in *Saccharina latissima*. Mar. Ecol. Prog. Ser. **630**: 25–39. doi:10.3354/meps13133
- Oliver, E. C. J., and others. 2021. Marine heatwaves. Ann. Rev. Mar. Sci. 13: 313–342.
- Pecl, G. T., and others. 2017. Biodiversity redistribution under climate change: Impacts on ecosystems and human wellbeing. Science **355**: eaai9214. doi:10.1126/science.aai9214
- Ross, F., P. Tarbuck, and P. I. Macreadie. 2022. Seaweed afforestation at large-scales exclusively for carbon sequestration: Critical assessment of risks, viability and the state of knowledge. Front. Mar. Sci. **9**: 1015612.
- Saha, M., and others. 2020. Response of foundation macrophytes to near-natural simulated marine heatwaves. Glob. Chang. Biol. **26**: 417–430.
- Sambhwani, K., G. Mathukiya, P. S. Dawange, R. A. Sequeira, K. Prasad, and V. A. Mantri. 2022. Analysis of functional traits in *Gracilaria dura* (Rhodophyta: Gracilariacae) reveals variation in wild and farmed populations. J. Appl. Phycol. **34**: 1017–1031. doi:10. 1007/s10811-022-02697-z
- Schmidt, A. L., J. K. C. Wysmyk, S. E. Craig, and H. K. Lotze. 2012. Regional-scale effects of eutrophication on ecosystem structure and services of seagrass beds. Limnol. Oceanogr. **57**: 1389–1402. doi:10.4319/lo.2012.57.5.1389
- Sockett, R. E. 2009. Predatory lifestyle of Bdellovibrio bacteriovorus. Annu. Rev. Microbiol. **63**: 523–539.
- Smale, D. A., and others. 2019. Marine heatwaves threaten global biodiversity and the provision of ecosystem services. Nat. Clim. Change. **9**: 306–312.
- Smith, K. E., and others. 2023. Biological impacts of marine heatwaves. Ann. Rev. Mar. Sci. **15**: 119–145.
- Teagle, H., S. J. Hawkins, P. J. Moore, and D. A. Smale. 2017. The role of kelp species as biogenic habitat formers in coastal marine ecosystems. J. Exp. Mar. Biol. Ecol. **492**: 81–98. doi:10.1016/j.jembe.2017.01.017
- Teichberg, M., and others. 2010. Eutrophication and macroalgal blooms in temperate and tropical coastal waters: Nutrient enrichment experiments with *Ulva* spp. Glob. Chang. Biol. **16**: 2624–2637. doi:10.1111/j.1365-2486. 2009.02108.x
- Thornton, D. C. O. 2014. Dissolved organic matter (DOM) release by phytoplankton in the contemporary and future ocean. Eur. J. Phycol. **49**: 20–46. doi:10.1080/09670262. 2013.875596

Jiang et al.

- Wada, S., M. N. Aoki, A. Mikami, T. Komatsu, Y. Tsuchiya, T. Sato, H. Shinagawa, and T. Hama. 2008. Bioavailability of macroalgal dissolved organic matter in seawater. Mar. Ecol. Prog. Ser. **370**: 33–44. doi:10.3354/meps07645
- Wada, S., S. Agostini, B. P. Harvey, Y. Omori, and J. M. Hall-Spencer. 2021. Ocean acidification increases phytobenthic carbon fixation and export in a warm-temperate system. Estuar. Coast Shelf Sci. 250: 107113. doi:10.1016/j.ecss.2020.107113
- Wang, C., W. D. Guo, Y. Li, R. A. Dahlgren, X. H. Guo, L. Y. Qu, and W. Zhuang. 2021. Temperature-regulated turnover of chromophoric dissolved organic matter in global dark marginal basins. Geophys. Res. Lett. 48: e2021GL094035. doi:10.1029/2021GL094035
- Wang, L. Q., X. Wang, Y. Y. Song, L. H. Sun, X. M. Chen, J. Q. Wu, C. H. Song, and Y. Zhao. 2022. Slowed down nitrogen mineralization under bacterial community-driven conditions by adding inhibitors during rice straw composting. Bioresour. Technol. **362**: 127778.
- Wang, Y., Y. Feng, H. Wang, M. Zhong, W. Chen, and H. Du. 2016. Physiological and proteomic analyses of two *Gracilaria lemaneiformis* strains in response to high-temperature stress. J. Appl. Phycol. **28**: 1847–1858. doi:10. 1007/s10811-015-0723-1
- Watanabe, K., G. Yoshida, M. Hori, Y. Umezawa, H. Moki, and T. Kuwae. 2020. Macroalgal metabolism and lateral carbon flows can create significant carbon sinks. Biogeosciences **17**: 2425–2440. doi:10.5194/bg-17-2425-2020
- Xu, F. Q., and H. W. Xue. 2019. The ubiquitin-proteasome system in plant responses to environments. Plant Cell Environ. **42**: 2931–2944.
- Yang, Y. F., X. G. Fei, J. M. Song, H. Y. Hu, G. C. Wang, and I. K. Chung. 2006. Growth of *Gracilaria lemaneiformis* under different cultivation conditions and its effects on nutrient removal in Chinese coastal waters. Aquaculture 254: 248– 255. doi:10.1016/j.aquaculture.2005.08.029
- Yao, Y. L., J. J. Wang, J. J. Yin, and X. Q. Zou. 2020. Marine heatwaves in China's marginal seas and adjacent offshore waters: Past, present, and future. J. Geophys. Res. Oceans **125**: e2019JC015801. doi:10.1029/2019JC015801

- Yu, J., and Y. F. Yang. 2008. Physiological and biochemical response of seaweed *Gracilaria lemaneiformis* to concentration changes of N and P. J. Exp. Mar. Biol. Ecol. **367**: 142–148. doi:10.1016/j.jembe.2008.09.009
- Zhao, Z., M. Gonsior, P. Schmitt-Kopplin, Y. C. Zhan, R. Zhang, N. Z. Jiao, and F. Chen. 2019. Microbial transformation of virus-induced dissolved organic matter from picocyanobacteria: Coupling of bacterial diversity and DOM chemodiversity. ISME J. **13**: 2551–2565. doi:10.1038/s41396-019-0449-1
- Zheng, Q., and others. 2019. Molecular characteristics of microbially mediated transformations of *Synechococcus*-derived dissolved organic matter as revealed by incubation experiments. Environ. Microbiol. **21**: 2533–2543. doi:10. 1111/1462-2920.14646
- Zlotnik, I., and Z. Dubinsky. 1989. The effect of light and temperature on DOC excretion by phytoplankton. Limnol. Oceanogr. **34**: 831–839.

Acknowledgments

This work was supported by the National Natural Science Foundation of China (42076154), the Natural Science Foundation of Fujian Province (2022 J01026 and 2021 J01026), the Marine Economic Development Special Fund Project of Fujian Province of China (FJHJF-L-2022-2111), the Royal Society China–UK International Exchanges grant "Effects of ocean acidification and warming in coastal systems (IEC\NSFC\181187)," and the MEL Internal Research Program (MELRI2304), and contributes to the Scientific Committee on Oceanic Research Changing Oceans Biological Systems project (OCE-1840868). The authors are grateful to the laboratory technicians Wenyan Zhao and Xianglan Zeng for their logistical and technical support.

Conflict of Interest

None declared.

Submitted 21 June 2023 Revised 24 August 2023 Accepted 14 December 2023

Associate editor: Birte Matthiessen